Phosphorylation of CSF-1R Y721 mediates its association with PI3K to regulate macrophage motility and enhancement of tumor cell invasion

Natalia G. Sampaio[1], Wenfeng Yu[2], Dianne Cox[3], Jeffrey Wyckoff[3,4], John Condeelis[3,4], E. Richard Stanley[2] and Fiona J. Pixley[1,*]

[1]School of Medicine and Pharmacology, University of Western Australia, Crawley, Western Australia 6009, Australia
[2]Department of Developmental and Molecular Biology, Albert Einstein College of Medicine, 1300 Morris Park Avenue, Bronx, NY 10461, USA
[3]Department of Anatomy and Structural Biology, Albert Einstein College of Medicine, 1300 Morris Park Avenue, Bronx, NY 10461, USA
[4]Gruss Lipper Biophotonics Center, Albert Einstein College of Medicine, 1300 Morris Park Avenue, Bronx, NY 10461, USA
*Author for correspondence (fiona.pixley@uwa.edu.au)

Accepted 1 February 2011
Journal of Cell Science 124, 2021-2031

doi:10.1242/jcs.075309

Summary

Colony stimulating factor-1 (CSF-1) regulates macrophage morphology and motility, as well as mononuclear phagocytic cell proliferation and differentiation. The CSF-1 receptor (CSF-1R) transduces these pleiotropic signals through autophosphorylation of eight intracellular tyrosine residues. We have used a novel bone-marrow-derived macrophage cell line system to examine specific signaling pathways activated by tyrosine-phosphorylated CSF-1R in macrophages. Screening of macrophages expressing a single species of CSF-1R with individual tyrosine-to-phenylalanine residue mutations revealed striking morphological alterations upon mutation of Y721. M–/–.Y721F cells were apolar and ruffled poorly in response to CSF-1. Y721-*P*-mediated CSF-1R signaling regulated adhesion and actin polymerization to control macrophage spreading and motility. Moreover, the reduced motility of M–/–.Y721F macrophages was associated with their reduced capacity to enhance carcinoma cell invasion. Y721 phosphorylation mediated the direct association of the p85 subunit of phosphoinositide 3-kinase (PI3K) with the CSF-1R, but not that of phospholipase C (PLC) γ2, and induced polarized PtdIns(3,4,5)P_3 production at the putative leading edge, implicating PI3K as a major regulator of CSF-1-induced macrophage motility. The Y721-*P*-motif-based motility signaling was at least partially independent of both Akt and increased Rac and Cdc42 activation but mediated the rapid and transient association of an unidentified ~170 kDa phosphorylated protein with either Rac-GTP or Cdc42-GTP. These studies identify CSF-1R-Y721-*P*–PI3K signaling as a major pathway in CSF-1-regulated macrophage motility and provide a starting point for the discovery of the immediate downstream signaling events.

Key words: Receptor tyrosine kinase, CSF-1R, PI3K, Macrophage motility

Introduction

Colony stimulating factor-1 (CSF-1) is the primary growth factor regulating the proliferation and differentiation of cells of the mononuclear phagocytic lineage (Pixley and Stanley, 2004). In addition, it is a crucial regulator of macrophage morphology and motility and acts as a chemotactic factor in inflammatory foci (Pixley and Stanley, 2004; Chitu and Stanley, 2006). Migratory macrophages are essential for normal development and immune function but also play a deleterious role in several diseases, including autoimmune diseases and rheumatoid arthritis (Chitu and Stanley, 2006), atherosclerosis (Fougerat et al., 2009) and obesity (Weisberg et al., 2003). CSF-1 has been directly implicated in the exacerbation of some of these diseases (Pixley and Stanley, 2004; Chitu and Stanley, 2006). Most notably, CSF-1 has been shown to promote tumor invasion and metastasis through interaction of tumor-associated macrophages and carcinoma cells mediated by a CSF-1-EGF paracrine loop (Wyckoff et al., 2004; Goswami et al., 2005; Condeelis and Pollard, 2006).

CSF-1 signals through the CSF-1 receptor tyrosine kinase (CSF-1R), which contains a split kinase domain and a number of intracellular tyrosine residues that are phosphorylated upon activation of the receptor (Yu et al., 2008). Phosphorylation of most of these tyrosine residues creates docking sites for a variety of signaling molecules to specifically mediate the pleiotrophic effects of CSF-1 (Pixley and Stanley, 2004). Previous studies examining the association of downstream signaling molecules with specific phosphorylated tyrosine motifs in the CSF-1R have used either ectopic expression of tyrosine-to-phenylalanine (Y-to-F) CSF-1R mutants in cells lacking an endogenous CSF-1R or expressed chimeric Y-to-F CSF-1R molecules with a heterologous extracellular domain (ECD) in CSF-1R-expressing myeloid cells (Pixley and Stanley, 2004). Such approaches have identified the CSF-1R association with Src family kinases (SFKs) through Y559-*P* (Rohde et al., 2004; Takeshita et al., 2007), the p85 subunit of phosphoinositide 3-kinase (PI3K) through Y721-*P* (Reedijk et al., 1992) and Cbl through Y974-*P* (Mancini et al., 2002; Wilhelmson et al., 2002). However, fully differentiated macrophages express specific motility-regulating proteins or splice variants not found in other cell types, including immature myeloid cells (Pixley et al., 1995; Pixley and Stanley, 2004). To study the pleiotrophic CSF-1R signaling pathways in a macrophage context, we have developed a bone-marrow-derived macrophage (BMM) cell line system that permits analysis of individual CSF-1R signaling pathways (Yu et al., 2008). This granulocyte macrophage CSF (GM-CSF)-dependent and CSF-1R-deficient MacCsf1r–/– (M–/–) cell line, when engineered to retrovirally express the wild-type (WT) CSF-1R

(M–/–.WT cells), is proliferation competent, differentiated and displays the well-spread bipolar morphology of control macrophages when grown in the presence of CSF-1 (Yu et al., 2008). Although retroviral expression of a number of individual Y-to-F mutant receptor molecules in M–/– cells each produced subtle morphological alterations, the most striking changes have been noted in M–/–.Y706F, M–/–.Y721F and M–/–.Y974F cell lines (Yu et al., 2008).

The Y721-*P*-based motif in the kinase insert of the CSF-1R has been demonstrated to mediate association with a number of signaling molecules (Pixley and Stanley, 2004), two of which, PI3K (Reedijk et al., 1992) and phospholipase C (PLC) γ2 (Bourette et al., 1997), are implicated in cell migration control. PI3K might also associate indirectly with the CSF-1R through either SFKs at Y559-*P* or Cbl at Y974-*P* (Pixley and Stanley, 2004). Class IA PI3Ks consist of a catalytic subunit (p110α, p110β and p110δ) complexed with a p85 regulatory subunit that translocates to activated receptor tyrosine kinases (RTKs) through interaction of its SH2 domains with phosphorylated YxxM motifs (Y^{721}VEM in the case of CSF-1R) (Reedijk et al., 1992; Faccio et al., 2007). Upon binding the RTK, p85 PI3K undergoes a conformational change to activate p110 (Wu et al., 2007) and produce phosphatidylinositol (3,4,5)-triphosphate [PtdIns(3,4,5)P_3] at the cell membrane. PI3K-regulated PtdIns(3,4,5)P_3 production activates a plethora of signals for growth, survival, proliferation and migration by inducing the translocation of pleckstrin homology (PH)-domain-containing molecules, such as Akt (PKB) and regulators of Rho family GTPases (Hawkins et al., 2006; Kolsch et al., 2008). Macrophages express each of the p110 PI3K isoforms, which have non-redundant biological roles in different cell types. Although there are differences in the CSF-1R recruitment of p110 PI3K isoforms between primary and immortalized macrophages, p110δ appears to be the main regulator of migration in both primary BMMs and BAC1.2F5 macrophages (Papakonstanti et al., 2008). PI3K signals primarily through Akt, leading to Rac activation and Rho inactivation, to stimulate actin polymerization, cytoskeletal remodeling and cell adhesion (Papakonstanti et al., 2008). Using a chimeric CSF-1R with an erythropoietin ECD, direct association of PI3K through Y721-*P* was found to be dispensable for signaling to the cytoskeleton in osteoclast precursors and BMMs, although PI3K activity was essential for remodeling and migration, suggesting that indirect association of PI3K with the CSF-1R is sufficient for motility signaling, at least in osteoclast precursors (Faccio et al., 2007).

PLCγ has two isoforms, PLCγ1 and PLCγ2, both of which are expressed in BMMs (Cheeseman et al., 2006). Similar to PI3K, the PLCγ isoforms function non-redundantly with PLCγ1 regulating phagocytosis (Cheeseman et al., 2006), whereas PLCγ2 signals downstream of CSF-1R to trigger differentiation in myeloid progenitor cells (Jack et al., 2009). Although PLCγ1 has been shown to regulate chemotaxis and adhesion in other cell types (van Rheenen et al., 2007) and PLCγ2 is important in osteoclast adhesion and migration (Epple et al., 2008), their roles in CSF-1-stimulated macrophage motility are not clear. Both isoforms are activated by tyrosine phosphorylation and membrane translocation that is induced by the association of the PLCγ SH2 domains with specific phosphorylated tyrosine motifs on RTKs, and the PLCγ PH domains with PtdIns(3,4,5)P_3 (Wilde and Watson, 2001). PLCγ2, but not PLCγ1, has been shown to associate with the CSF-1R in a yeast two-hybrid assay, and the interaction was at least partially dependent on Y721-*P*, although this could not be confirmed in vivo (Bourette et al., 1997). Importantly, the RTK phosphorylated tyrosine motifs mediating binding of the PLCγ SH2 domain differ from the p85-PI3K-preferred YxxM motif (Songyang et al., 1993).

Here, we demonstrate that loss of Y721-*P*-based signaling from the CSF-1R in macrophages substantially inhibits their capacity to ruffle, spread and migrate owing to disruption of the ability to form phosphorylated-paxillin-rich adhesion structures and disruption in actin polymerization. The capacity of these macrophages to promote carcinoma cell invasion is also reduced. We show that the Y721-*P* motif mediates the association of PI3K, but not PLCγ, with the activated CSF-1R and that CSF-1-induced PI3K activation is substantially reduced in the absence of this association.

Results

Y721-*P*-based CSF-1R signaling regulates macrophage morphology

M–/–.WT and M–/–.Y721F macrophages were grown in the continuous presence of CSF-1 for at least 1 week after thawing from GM-CSF-maintained stocks. During that time, the cells became substantially more spread and adherent (data not shown). After plating onto fibronectin-coated coverslips for 2 days, subconfluent growing cells were fixed and examined using scanning electron microscopy (SEM) (Fig. 1A). M–/– cells expressing the WT CSF-1R resembled normal macrophages (Yu et al., 2008) and were elongated with a ruffled leading lamellipodium. By contrast, a putative leading edge was usually difficult to discern in the apolar M–/–.Y721F cells and these cells bore very few ruffles but displayed many filopodia (Fig. 1A). In addition, M–/–.Y721F cells appeared flatter with an enlarged area of attachment. Quantification of the footprint area (Fig. 1B) and elongation ratio (Fig. 1C) confirmed these impressions. By contrast, cell size was not substantially increased in the mutant macrophages, as measured by flow cytometric forward scatter (FSC) analysis [M–/–.WT=100,733±26,948; M–/–.Y721F=102,211±30,559 (mean FSC±s.d.)] (Fig. 1D). Thus, the increased footprint area in M–/–.Y721F macrophages was not secondary to an increase in cell volume. Because dorsal ruffling is maximally stimulated within 3 minutes of CSF-1 stimulation (Boocock et al., 1989), SEM was repeated on cells stimulated for 3 minutes. CSF-1 stimulated minimal ruffling in M–/–.Y721F cells compared with that in M–/–.WT cells (Fig. 1E). Thus, loss of signaling from Y721-*P* reduces macrophage ruffling and elongation while increasing footprint area.

Y721-*P*-based CSF-1R signaling regulates paxillin phosphorylation and incorporation into adhesion structures

Given that M–/–.Y721F macrophages had a larger attachment area than control macrophages, their ventral surface adhesion structures were examined by immunofluorescent staining for paxillin Y118-*P* using total internal reflection (TIRF) microscopy (Pixley et al., 2005). Macrophages, being highly motile cells, do not form large stable focal adhesions but produce small linear focal complexes at the periphery and dot-like point contacts under the entire ventral surface of the cell (Pixley and Stanley, 2004). To capture peak adhesion, cells were starved of CSF-1 overnight before re-addition of CSF-1 for 15 minutes (Pixley et al., 2001). Despite their increased footprint area, M–/–.Y721F cells displayed fewer and less intensely paxillin-Y118-*P*-stained adhesion structures than did control cells (Fig. 2A). Moreover, they rarely formed the linear focal complexes commonly found in M–/–.WT cells (Fig. 2A,

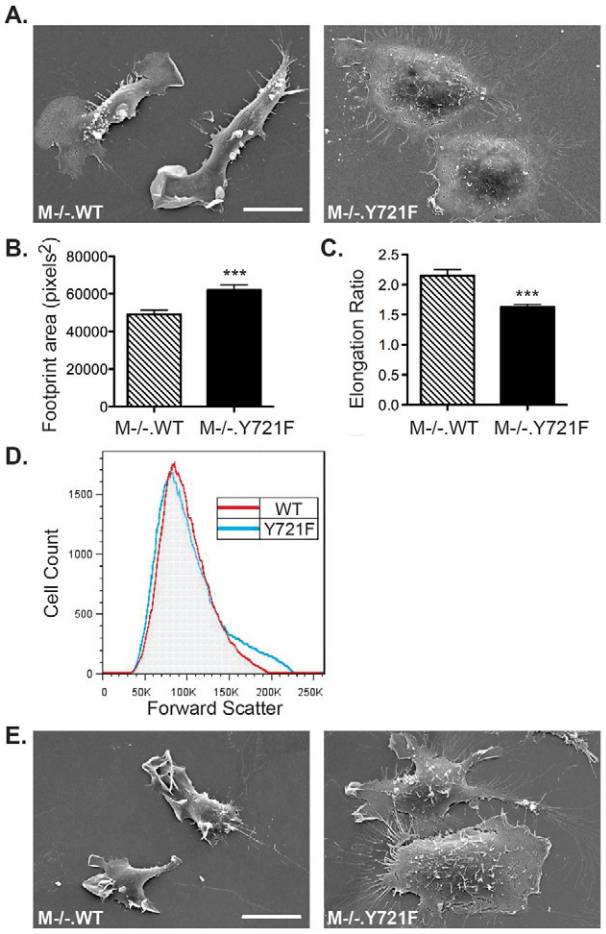

Fig. 1. M–/–.Y721F macrophages display altered morphology. SEM images of M–/–.WT and M–/–.Y721F macrophages plated onto fibronectin-coated coverslips for 2 days and either kept in the continuous presence of CSF-1 (**A**) or incubated without growth factor overnight prior to stimulation with 120 ng/ml CSF-1 for 3 minutes (**E**) before fixation. Scale bars: 20 µM. M–/–.WT and M–/–.Y721F macrophages plated onto fibronectin-coated coverslips and grown in the continuous presence of CSF-1 were also fixed and stained for F-actin before cell outline tracing to measure the cell footprint area (**B**) and elongation ratio (maximum length:maximum width) (**C**). Data are means±s.e.m. ($n \geq 40$). ***$P<0.001$. (**D**) Forward scatter analysis of M–/–.WT and M–/–.Y721F cell size (FACSCantoII, BD Biosciences).

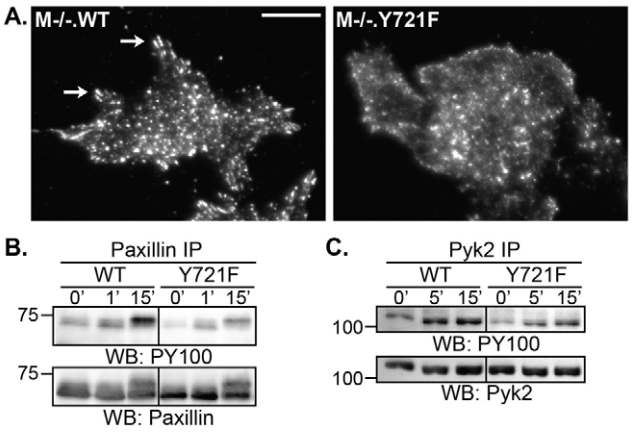

Fig. 2. Paxillin and Pyk2 phosphorylation, and the incorporation of paxillin into adhesion structures, are reduced in M–/–.Y721F macrophages. (**A**) M–/–.WT and M–/–.Y721F macrophages were plated onto fibronectin-coated coverslips and incubated without growth factor overnight before stimulation with 120 ng/ml CSF-1 for 15 minutes followed by fixation, staining and examination by TIRF microscopy for adhesion structures rich in paxillin Y118-*P*. Scale bar: 20 µM. Lysates from CSF-1-starved M–/–.WT and M–/–.Y721F macrophages stimulated with 120 ng/ml CSF-1 for the indicated times were subjected to paxillin (**B**) or Pyk2 (**C**) immunoprecipitation (IP) then immunoblotted (WB) for the indicated proteins.

arrows). Consistent with the immunofluorescent results, western blotting of paxillin immunoprecipitates for phosphorylated tyrosine (PY100) from mutant and control cell lysates stimulated with CSF-1 for 0, 1 or 15 minutes demonstrated reduced tyrosine phosphorylation of paxillin in the mutant cells (Fig. 2B). Paxillin constitutively binds Pyk2, an adhesion kinase that is highly expressed in macrophages and phosphorylates paxillin to regulate macrophage adhesion and motility (Owen et al., 2007). Pyk2 is tyrosine phosphorylated and activated in response to CSF-1 (Owen et al., 2007; Pixley and Stanley, 2004) and PY100 immunoblotting of Pyk2 immunoprecipitates revealed reduced phosphorylation in the mutant cells (Fig. 2C). Thus, CSF-1R signaling to mediate adhesion, through Pyk2 activation and paxillin phosphorylation, is substantially reduced in M–/–.Y721F cells.

Y721-*P*-based signaling regulates adhesion gene expression

Macrophages grown exclusively in GM-CSF are poorly spread and apolar (Fig. 3A); these cells display a monocyte–macrophage phenotype mixed with some dendritic cell characteristics (F4/80^{hi} Mac-1^{+} Gr1^{-} CD11c^{+}) (Yu et al., 2008). All macrophage cultures used here were exposed to CSF-1 for at least 1 week to induce the differentiated macrophage phenotype shown in Fig. 3A (F4/80^{hi} Mac-1^{hi} Gr1^{lo} CD11c^{lo}) (Yu et al., 2008). The CSF-1-induced differentiation results in increased expression of molecules that regulate macrophage adhesion and motility, including the adhesion kinases FAK and Pyk2, as well as an adhesion phosphatase PTPϕ (also known as PTPRO) (F.J.P., unpublished). FAK and Pyk2 phosphorylate paxillin in response to CSF-1, whereas PTPϕ dephosphorylates it (Owen et al., 2007; Pixley et al., 2001). Because adhesion and motility are affected by mutation of Y721, we investigated whether loss of the Y721-*P* motif influenced this long-term CSF-1 effect on gene expression. Immunoblotting of lysates from M–/–.WT and M–/–.Y721F cells indicated that there was a clear increase in PTPϕ, particularly the smaller 43 kDa splice variant, and a possible increase in FAK, but no change in Pyk2 protein expression in the mutant macrophages (Fig. 3B). To examine whether any alterations in protein expression were due to increased transcription, quantitative real-time PCR (qRT-PCR) was performed for the three genes in cells grown continuously in the presence of CSF-1. Consistent with the protein expression profile, the levels of mRNA encoding PTPϕ were substantially increased (~2.5-fold), whereas those encoding FAK were not substantially different and those for Pyk2 were not altered, in M–/–.Y721F cells compared with control cells (Fig. 3C). Thus, loss of signaling from Y721-*P* in continuously growing cultures alters the expression of PTPϕ, an important regulator of macrophage adhesion and motility (Pixley et al., 2001). These results indicate

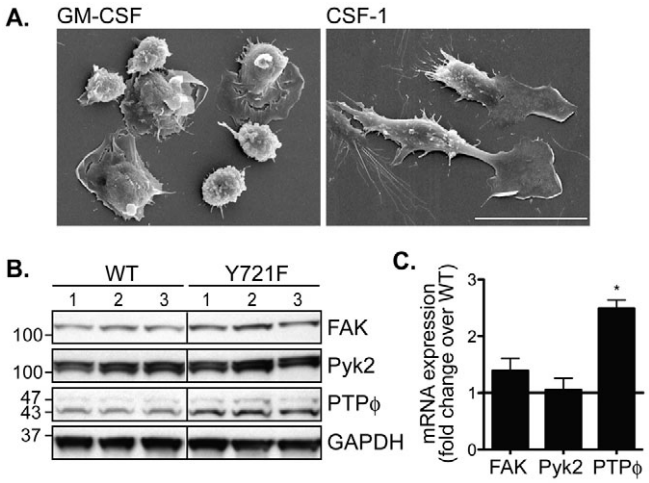

Fig. 3. Loss of CSF-1R Y721-*P* signaling increases expression of the adhesion-regulating PTPϕ. (**A**) SEM images of M–/–.WT macrophages grown in the continuous presence of either GM-CSF or CSF-1 for 1 week before plating on fibronectin-coated coverslips for 2 days. Scale bar: 20 µM. (**B**) M–/–.WT and M–/–.Y721F cell lysates were examined by SDS-PAGE and immunoblotting for the indicated proteins. (**C**) Levels of mRNA encoding FAK, Pyk2 and PTPϕ were examined in M–/–.WT and M–/–.Y721F macrophages cultured in the continuous presence of CSF-1 by qRT-PCR analysis. Results are expressed as fold-change in M–/–Y721F cell gene expression compared with that in M–/–.WT cells. The data are means±s.e.m. for three independent experiments. **P*<0.05.

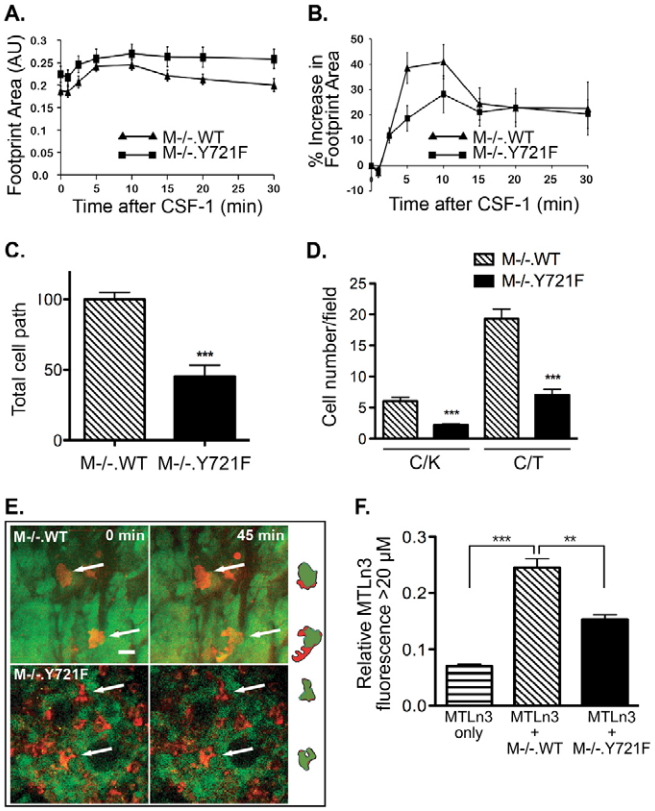

Fig. 4. CSF-1R Y721-*P* signaling regulates macrophage spreading, motility and promotion of carcinoma cell invasion. CSF-1-stimulated M–/–.WT (▲) and M–/–.Y721F (■) macrophages plated onto glass-bottomed dishes were examined by time-lapse video microscopy and their cell outlines traced. The mean (±s.e.m.) total footprint area (**A**) and relative (%) increase in footprint area (**B**) for 30 minutes after CSF-1 (120 ng/ml) addition is shown ($n \geq 40$). (**C**) Total path length was measured by centroid analysis at 2.5-minute intervals up to 1 hour after CSF-1 stimulation and means±s.e.m. calculated for 10 cells each. (**D**) Boyden chamber analysis of CSF-1-stimulated chemokinetic (C/K) and chemotactic (C/T) motility is shown. The data are normalized to the M–/–.WT C/K result and are means±s.e.m. for a representative experiment (n=3). (**E**) M–/–.WT and M–/–.Y721F cells labeled with Cell Tracker Red (red) were injected into GFP-expressing MTLn3 xenograft carcinomas (green) 24 hours prior to imaging by multiphoton microscopy for 45 minutes. Scale bar: 20 µM. Two M–/–.WT and M–/–.Y721F cell (arrows) outlines in the first (green) and last (red) frame were overlaid to evaluate cell motility in vivo. (**F**) CFP-expressing MTLn3 carcinoma cells were either cultured alone or co-cultured with M–/–.WT or M–/–.Y721F cells and their capacity to invade more than 20 µM into overlaying collagen after 24 hours measured. The data are means±s.e.m. ***P*<0.01; ****P*<0.001.

that Y721-*P*-based signaling not only regulates rapid ruffling and adhesion responses in macrophages but also affects longer term signaling responses, as reflected in changes in gene and protein expression.

Y721-*P*-based CSF-1R signaling regulates the macrophage spreading and motility response in vitro and in vivo

Cell spreading and motility require actin-polymerization-based membrane protrusion and phosphorylated tyrosine triggered adhesion, followed by actomyosin contractility (Gupton and Waterman-Storer, 2006). Given that Y721-*P*-based signaling regulates formation of adhesion structures rich in phosphorylated paxillin, we used time-lapse video microscopy to determine whether spreading and migration were altered by the reduced adhesion in mutant cells. M–/–.WT and M–/–.Y721F cells were starved of CSF-1 overnight then imaged during stimulation with CSF-1. To assess cell spreading, cell footprints were determined at 0, 1, 2.5, 5, 10, 15, 20 and 30 minutes (Fig. 4A). Although M–/–.Y721F cells displayed a larger footprint area at each time point examined, the spreading response to CSF-1 appeared attenuated in these cells (Fig. 4A). Indeed, when the percentage increase in footprint area after CSF-1 stimulation was calculated, M–/–.Y721F cells showed reduced spreading (28%) compared with M–/–.WT cells (41%) (Fig. 4B). In addition, the mutant cells failed to contract significantly after the maximal spread area was reached at ~10 minutes (Fig. 4A,B). Consistent with their attenuated spreading response to CSF-1, M–/–.Y721F cells also migrated more slowly than control cells in a uniform concentration of CSF-1 (Fig. 4C, see WT and Y721F cells in supplementary material Movies 1 and 2). To assess the effects of loss of signaling from Y721-*P* on chemotaxis towards CSF-1, Boyden chamber analysis was used. M–/–.Y721F cells displayed an ~63% reduction in chemotactic capacity towards CSF-1, with a similar affect on chemokinetic motility (Fig. 4D). To determine whether this marked in vitro reduction in CSF-1-induced motility was recapitulated in vivo, control or mutant macrophages labeled with Cell Tracker Red were injected into GFP-expressing MTLn3 rat mammary carcinoma cell xenograft tumors in SCID mice 24 hours before imaging. Two-color multiphoton microscopy was then used to image the macrophages (red) moving among tumor cells (green) for 1 hour. Although M–/–.WT macrophages could be observed moving in vivo, M–/–.Y721F cells did not display discernible movement during the course of the experiment (Fig. 4E). Thus, loss of

signaling from Y721-*P* of the CSF-1R leads to a striking reduction in macrophage motility in vitro and in vivo.

M–/–.Y721F macrophages promote less in vitro carcinoma cell invasion than M–/–.WT cells

We have previously shown that carcinoma cells co-cultured with macrophages show enhanced invasion into the ECM in vitro owing to the presence of a CSF-1-EGF paracrine 'dialogue' between the two cell types (Goswami et al., 2005). To determine whether macrophage motility is an important component of this promotion of tumor cell invasion, MTLn3 cells were co-cultured with either M–/–.WT or M–/–.Y721F macrophages and the degree of invasion by the carcinoma cells into overlaid collagen I matrix was determined. Carcinoma cells were only minimally invasive into collagen I in the absence of co-cultured macrophages (Fig. 4F). When they were co-cultured with control macrophages, there was a 3.5-fold increase in their invasive capacity, whereas there was only a 2-fold enhancement of their invasiveness in the presence of M–/–.Y721F cells (Fig. 4F). Thus, CSF-1R signaling from the Y721-*P* motif regulates not only macrophage motility but also the invasive capacity of carcinoma cells in co-culture.

Phosphorylation of Y721 mediates the association of PI3K, but not PLCγ, with CSF-1R

To identify CSF-1R signaling pathways activated downstream of Y721-*P*, a CSF-1R immunoprecipitation timecourse of the association of the CSF-1R with PI3K and PLCγ2 was performed (Fig. 5A). The kinetics of the CSF-1R tyrosine phosphorylation (PY100) was similar between the WT and Y721F receptors with peak phosphorylation at 2.5 minutes, which diminished significantly by 15 minutes (Fig. 5A, panel 1). In repeated experiments (n=3), the amount of tyrosine phosphorylation per unit of receptor protein for the Y721F receptor was ~70% that of the WT level. This is likely to be largely due to the absence of Y721 phosphorylation as Y721F has been shown to be a major tyrosine phosphorylation site (Reedijk et al., 1992) and the kinase activity of CSF-1R Y721F is comparable to that of the WT receptor (Yu et al., 2008). Indeed,

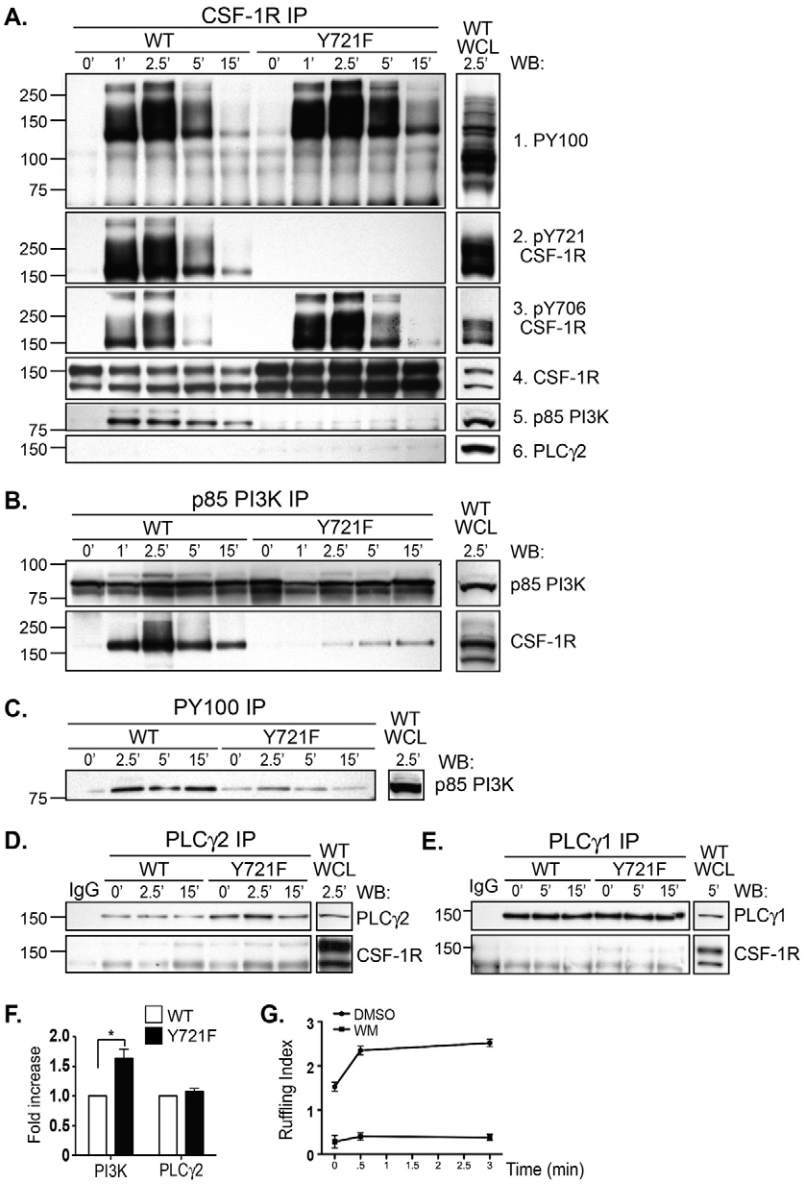

Fig. 5. Mutation of CSF-1R Y721 abrogates its association with p85 PI3K, but not PLCγ, and induces PI3K expression. CSF-1-starved M–/–.WT and M–/–.Y721F cells were stimulated with CSF-1 for the indicated times and lysates subjected to CSF-1R (**A**), p85 PI3K (**B**), PY100 (**C**), PLCγ2 (**D**) and PLCγ1 (**E**) immunoprecipitation (IP). Eluted proteins were subjected to SDS-PAGE and immunoblotting (WB) for the indicated proteins. WCL, whole-cell lysates. (**F**) qRT-PCR analysis of mRNA encoding p85 PI3K and PLCγ2 in M–/–.WT and M–/–.Y721F macrophages grown continuously in CSF-1. Results are the fold-change in M–/–Y721F cell gene expression compared with that in M–/–.WT cells (means±s.e.m. for three independent experiments). **P*<0.05. (**G**) CSF-1-starved M–/–.WT cells were treated with either 100 nM wortmannin or DMSO for 30 minutes before CSF-1 stimulation for the indicated times. F-actin-rich ruffles were visualized with Alexa-Fluor-568–phalloidin and quantified as described in the Materials and Methods.

CSF-1R Y706 phosphorylation was not affected by mutation of Y721 (Fig. 5A, panel 3; ~100% of WT).

To investigate whether the lack of Y721 phosphorylation affected the association of the putative mediators of macrophage motility, the presence of co-immunoprecipitated p85 PI3K and PLCγ2 was examined by immunoblotting. Strikingly, whereas p85 PI3K rapidly and strongly associated with the WT CSF-1R upon CSF-1 stimulation, with peak association at ~2.5 minutes, its association with the Y721F receptor was at background levels, despite receptor overloading (Fig. 5A, panel 5). To confirm that the induced association of PI3K with the CSF-1R was mediated by Y721-*P*, reciprocal PI3K immunoprecipitations were performed (Fig. 5B). Although the WT receptor rapidly, strongly and transiently associated with PI3K upon CSF-1 stimulation, with a peak at 2.5 minutes, CSF-1R Y721F association with PI3K was delayed and very weak (Fig. 5B, lower panel). Taken together, the CSF-1R and PI3K co-immunoprecipitation results suggest that, in the absence of Y721-*P*, the PI3K–CSF-1R association is very weak and significantly delayed. Indeed, the PI3K–CSF-1R-Y721F association is likely to be indirect, mediated by either SFKs at Y559-*P* or Cbl at Y974-*P* (Herrera-Velit and Reiner, 1996; Faccio et al., 2007). Moreover, p85 PI3K levels were strikingly reduced in the PY100 immunoprecipitations (Fig. 5C) in CSF-1 stimulated M–/–.Y721F cells compared with those in M–/–.WT cells. Thus, CSF-1R requires Y721 to support association of p85 PI3K in response to CSF-1.

Phosphorylation of Y721 has also been reported to trigger receptor association with PLCγ2 in a yeast two-hybrid approach using an immature myeloid cell line (Bourette et al., 1997). However, PLCγ2 did not exhibit substantial CSF-1-induced association with CSF-1R in fully differentiated macrophages (Fig. 5A, panel 6) and reciprocal PLCγ2 immunoprecipitations demonstrated weak association of both WT and Y721F receptors with PLCγ2 (Fig. 5D). Thus, in contrast to PI3K, the association of PLCγ2 with the CSF-1R is not dependent upon Y721. PLCγ1 immunoprecipitations also demonstrated a weak Y721-*P*-independent association of PLCγ1 with CSF-1R (Fig. 5E). In addition, in cells cultured continuously in CSF-1, qRT-PCR analysis revealed an increase in the level of mRNA encoding p85 PI3K in M–/–.Y721F cells with no change in PLCγ2 expression (Fig. 5F), consistent with a possible compensatory transcriptional response to overcome reduced PI3K activation in M–/–.Y721F cells. These findings suggest that the Y721-*P* motif is a crucial regulator of the CSF-1R association with PI3K, but not that of PLCγ1 or PLCγ2.

To determine whether the association of PI3K with CSF-1R has functional consequences in our model system, the effect of inhibition of PI3K activity by wortmannin on CSF-1-induced ruffling response was examined. We have previously shown that CSF-1 induces ruffling in RAW264.7 macrophages in a PI3K-dependent manner (Kheir et al., 2005). CSF-1 was removed from M–/–.WT cells overnight before treatment with either 100 nM wortmannin or DMSO for 30 minutes followed by CSF-1 stimulation for 0, 0.5 or 3 minutes. Cells were stained for F-actin and scored for ruffling, as previously described (Kheir et al., 2005; Abou-Kheir et al., 2008). CSF-1 induced ruffling in control cells in a rapid and sustained manner, whereas wortmannin abrogated the CSF-1-induced ruffling response altogether, as well as the serum-induced baseline ruffling seen in DMSO-treated cells (Fig. 5G). Thus, PI3K mediates CSF-1-induced ruffling in macrophages.

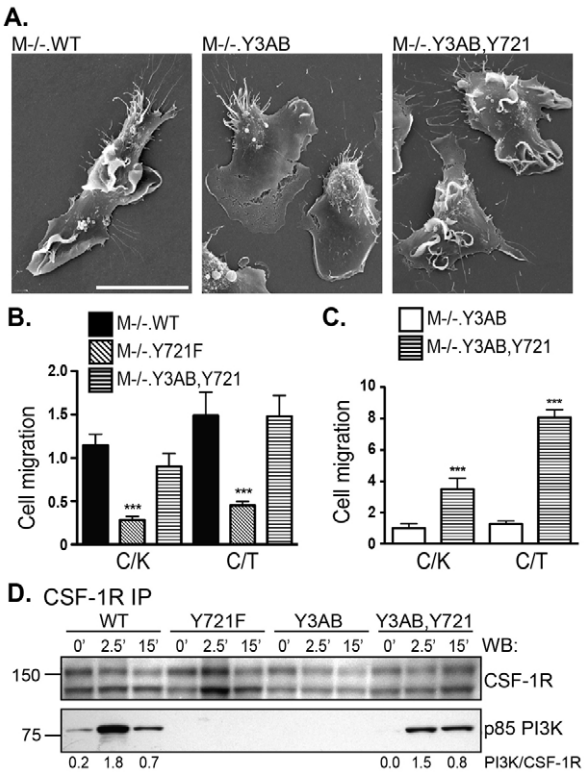

Fig. 6. The CSF-1R Y721-*P* motif is necessary and sufficient for CSF-1-induced ruffling and chemotaxis, as well as association of p85 PI3K and CSF-1R. (**A**) SEM images of M–/–.WT, M–/–.Y721F and M–/–.Y3AB,Y721 macrophages plated onto fibronectin-coated coverslips. Cells were incubated without growth factor overnight before stimulation with 120 ng/ml CSF-1 for 3 minutes. Scale bar: 20 μM. Boyden chamber analysis of CSF-1-stimulated chemokinetic (C/K) and chemotactic (C/T) motility in M–/–.WT, M–/–.Y721F and M–/–.Y3AB,Y721 macrophages (**B**) or in M–/–.Y3AB and M–/–.Y3AB,Y721 macrophages (**C**). Data are means±s.e.m. for a representative experiment (n=3). $^{**}P<0.01$; $^{***}P<0.001$. (**D**) CSF-1R immunoprecipitations (IP) of lysates from CSF-1-starved M–/–.WT, M–/–.Y721F, M–/–.Y544,Y559,Y807 and M–/–.Y3AB,Y721 cells, incubated without growth factor overnight before stimulation with 120 ng/ml CSF-1 for the indicated times, were examined for associated p85 PI3K following SDS-PAGE. The numbers below the blot indicate the relative levels of co-immunoprecipitated PI3K, as determined by densitometry.

Add-back of Y721 to the CSF-1R restores ruffling, chemotaxis and PI3K association

We have previously shown that mutation of all eight tyrosine residues phosphorylated in activated CSF-1R causes complete loss of CSF-1R signaling in response to CSF-1 and that Y559 and Y897 play a crucial role in macrophage survival, proliferation and differentiation (Yu et al., 2008). Adding back these two tyrosine residues and Y544 creates an ‘add-back’ (AB) receptor (CSF-1R Y544,559,807) that restores CSF-1R kinase activity and CSF-1-regulated macrophage proliferation, but not normal CSF-1-regulated morphology (W.Y., F.J.P., E.R.S., unpublished results). Similar to M–/–.Y721F cells, M–/–.Y544,559,807AB (M–/–.Y3AB) cells did not ruffle substantially after CSF-1 stimulation (Fig. 6A). Restoration of Y721 to this triple AB receptor (M–/–.Y3AB,Y721) in macrophages restored the CSF-1-regulated ruffling response (Fig. 6A). Moreover, addition of Y721 to the 3AB receptor partially

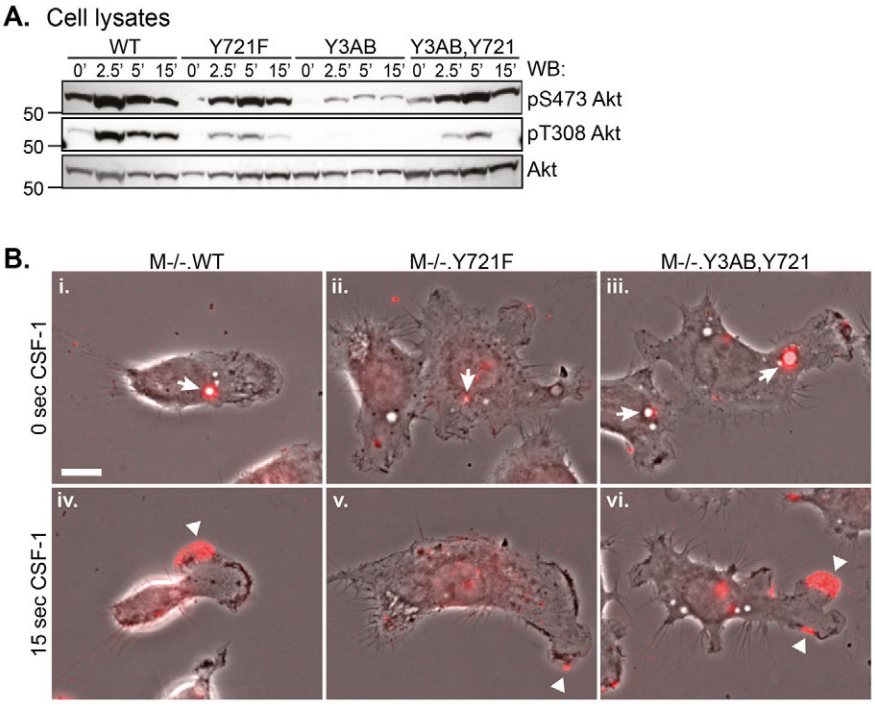

Fig. 7. PI3K association with the CSF-1R through Y721-*P* regulates Akt activation and PtdIns(3,4,5)P_3 production. (**A**) M–/–.WT, M–/–.Y721F, M–/–.Y544,Y559,Y807 and M–/–.Y3AB,Y721 cells were stimulated with 120 ng/ml CSF-1 and their lysates examined for Akt S473 or T308 phosphorylation. (**B**) M–/–.WT, M–/–.Y721F and M–/–.Y3AB,Y721 cells plated onto fibronectin-coated coverslips were incubated without growth factor overnight before stimulation with 120 ng/ml CSF-1 for 0 or 15 seconds and were then subjected to simultaneous fixation and extraction with 3.7% paraformaldehyde, 0.1% glutaraldehyde and 0.15 mg/ml saponin to examine CSF-1-induced PtdIns(3,4,5)P_3 production. Representative merged images consist of PtdIns(3,4,5)P_3 (red) and phase-contrast (grayscale) images of M–/–.WT (i,iv), M–/–.Y721F (ii,v) and M–/–.Y3AB,Y721 (iii,vi) cells treated with CSF-1 for 0 (i–iii) or 15 (iv–vi) seconds. Arrows indicate PtdIns(3,4,5)P_3-encircled vesicles and arrowheads point to CSF-1-induced PtdIns(3,4,5)P_3 in lamellipodia. Images are representative of those in four independent experiments. Scale bar: 10 µM.

restored CSF-1-regulated chemokinesis and fully restored CSF-1-regulated chemotaxis when compared with that in M–/–.WT and M–/–.Y721F cells (Fig. 6B) or M–/–.Y3AB cells (Fig. 6C). To confirm whether Y721 is not only necessary but also sufficient for mediating PI3K association with the activated CSF-1R, CSF-1R immunoprecipitations of lysates from M–/–.WT, M–/–.Y721F, M–/–.Y3AB and M–/–.Y3AB,Y721 cells stimulated with CSF-1 for 0, 2.5 and 15 minutes were performed. As in the experiments described above, PI3K failed to associate with the mutant CSF-1R Y721F, as well as the CSF-1R Y3AB, but add-back of Y721 to the Y3AB receptor was sufficient to restore PI3K association with the receptor (Fig. 6D). Taken together, these results indicate that the Y721-*P* motif is necessary and sufficient for association of PI3K with the CSF-1R and that it is a crucial regulator CSF-1-mediated macrophage ruffling and chemotaxis.

The association of PI3K with CSF-1R Y721-*P* regulates Akt activation and PtdIns(3,4,5)P_3 production

Akt is a key effector of PI3K downstream of RTKs (Hawkins et al., 2006). PtdIns(3,4,5)P_3 production at the plasma membrane triggers Akt translocation and phosphorylation of T308 in the activation loop and S473 in the hydrophobic motif of the C-terminus, both of which are required for full activation of its kinase domain (Peifer and Alessi, 2008). To examine the role of Y721-*P*-based CSF-1R signaling in Akt activation, lysates from CSF-1-stimulated M–/–.WT, M–/–.Y721F, M–/–.Y3AB and M–/–.Y3AB,Y721 cells were examined for Akt S473-*P* and Akt T308-*P*. Phosphorylation of S473 was only delayed and decreased moderately in both M–/–.Y721F and M–/–.Y3AB,Y721 cells, compared with the severe reduction seen in M–/–.Y3AB cells (Fig. 7A, top panel). By contrast, the levels of Akt T308-*P* were more severely affected in M–/–.Y721F cells, with complete absence of phosphorylation in M–/–.Y3AB cells (Fig. 7A, middle panel). Add back of Y721 in M–/–.Y3AB,Y721 cells did not increase Akt phosphorylation on T308 beyond that seen in M–/–.Y721F cells. Thus, Y721 is important in the signaling for Akt activation, but other CSF-1R phosphorylated tyrosine residues are also required given that association of PI3K with the receptor is not sufficient for full Akt activation.

Because Akt activation is not restored in M–/–.Y3AB,Y721 cells, but they ruffle and chemotax in response to CSF-1, a monoclonal antibody against PtdIns(3,4,5)P_3 was used to examine PtdIns(3,4,5)P_3 levels and distribution in M–/–.WT, M–/–.Y721F and M–/–.Y3AB,Y721 cells upon CSF-1 stimulation (Yip et al., 2008). Ring-like PtdIns(3,4,5)P_3 staining around a subset of intracellular vesicles could be seen in both CSF-1-starved and stimulated cells (Fig. 7B, arrows), whereas non-vesicular PtdIns(3,4,5)P_3 staining was only seen infrequently in CSF-1-starved cells (Fig. 7Bi–iii). Within 15 seconds of CSF-1 stimulation, localized patches of strong PtdIns(3,4,5)P_3 staining were evident at the putative leading edge in M–/–.WT and M–/–.Y3AB,Y721 cells but not in M–/–.Y721F cells (Fig. 7Biv–vi). PtdIns(3,4,5)P_3 levels were also examined at 30 seconds and 3 minutes, by which time the signal was beginning to diminish (data not shown). Thus, association of PI3K with the CSF-1R through the Y721-*P* motif correlates with rapid CSF-1 stimulation of PtdIns(3,4,5)P_3 production at the putative leading edge where actin is polymerizing.

Actin polymerization is regulated by Y721-*P*-triggered CSF-1R signaling

The CSF-1R-Y721-*P*-specific activation of PI3K and its effect on PtdIns(3,4,5)P_3 production, macrophage ruffling and chemotaxis indicates that Y721-*P*-triggered PI3K signaling mediates CSF-1 regulation of macrophage motility. Although Akt could be one effector of the PI3K response downstream of Y721-*P*, a number of other PH-domain-containing effectors might also propagate the motility signal, including regulators of the Rho family GTPases (Hawkins et al., 2006). Of the Rho family GTPases expressed in macrophages, active Rac induces ruffling, focal complex formation and motility, whereas Cdc42 induces formation of filopodia

downstream of CSF-1 (Allen et al., 1997; Kheir et al., 2005). Rac and Cdc42 act by stimulating actin polymerization, with an initial increase in total F-actin at 30 seconds followed by a prolonged wave peaking around 3 minutes (Diakonova et al., 2002). Because M–/–.Y721F cells showed a very blunted ruffling response at 3 minutes, we examined CSF-1-stimulated actin polymerization in M–/–.WT and M–/–.Y721F cells. Surprisingly, although there was no effect on the actin polymerization wave that occurred at 3 minutes, the increase in F-actin content at 30 seconds was profoundly reduced in the mutant cells (Fig. 8A). Restoration of Y721-*P* signaling in M–/–.Y3AB,Y721 cells returned actin polymerization rates to normal levels (Fig. 8A). To examine the kinetics of Rac and Cdc42 activation in our cells, GST–PAK–CRIB pull-down assays were performed on M–/–.WT cells stimulated with CSF-1 for the indicated times (Fig. 8B). Interestingly, levels of active Rac and Cdc42 remained unchanged until well after the CSF-1-stimulated actin polymerization events, with a brief increase in activation seen at 5 minutes (Fig. 8B). To determine whether Rac or Cdc42 activation was reduced in M–/–.Y721F cells at the time of actin polymerization, pull-down assays were performed in CSF-1-stimulated M–/–.WT and M–/–.Y721F cells. We were unable to demonstrate reduced Rac or Cdc42 activation in the mutant cells following CSF-1 stimulation in repeated assays at 0 and 30 seconds (Fig. 8C, upper two panels) or at 3 minutes (data not shown). However, a PY100 immunoblot of the GST–PAK–CRIB pull-down samples revealed an ~170 kDa phosphorylated protein associating with either activated Rac or Cdc42 at 30 seconds and in M–/–.WT cells only (Fig. 8C, third panel). Re-probing the membrane for phosphorylated tyrosine residues at that approximate molecular mass, including CSF-1R (165 kDa), PLCγ1 (155 kDa), PLCγ2 (150 kDa), SHIP1 (145 kDa), IRS-2 (180 kDa) and four known Rac guanine-nucleotide-exchange factors (GEFs), TIAM (170–180 kDa), DOCK180 (180 kDa), DOCK2 (180 kDa) and Sos1 (170 kDa), failed to identify the protein (Fig. 8C; data not shown). Thus, Y721-*P*-based signaling regulates the CSF-1-induced rapid actin polymerization response but not Rac or Cdc42 activation at 30 seconds. At this early time point, in the absence of any detectable increase in active Rac or Cdc42, the activated Rac or Cdc42 complex transiently associates with an unidentified ~170 kDa tyrosine-phosphorylated protein in a Y721-*P*-dependent manner.

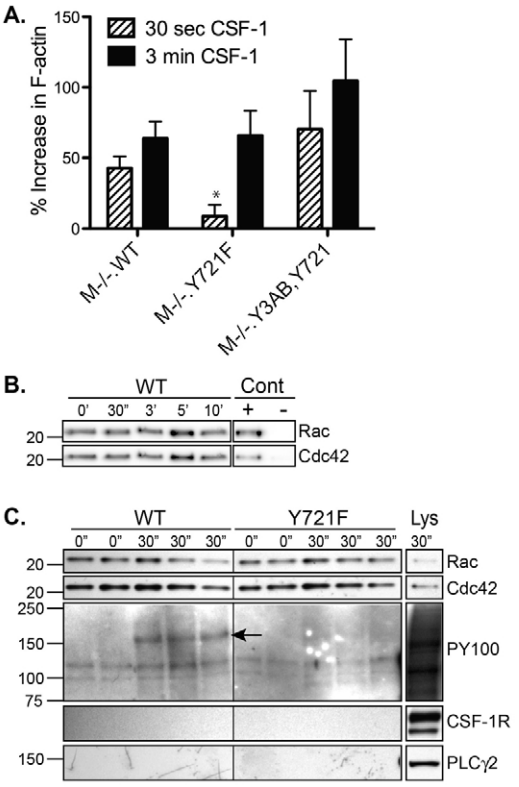

Fig. 8. The Y721-*P* motif triggers signaling that regulates the first peak of actin polymerization and the association of an ~170 kDa phosphorylated protein with a Rac-GTP or Cdc42-GTP complex. (**A**) Relative (%) increase in cellular F-actin content in CSF-1-starved M–/–.WT, M–/–.Y721F and M–/–.Y3AB,Y721 cells stimulated with 120 ng/ml CSF-1 for either 30 seconds or 3 minutes. The data are means±s.e.m. (n=4). *P<0.05. (**B**) CSF-1-starved M–/–.WT cells were stimulated with 120 ng/ml CSF-1 for the indicated times and lysates subjected to GST–PAK–CRIB pull down for Rac-GTP and Cdc42-GTP followed by SDS-PAGE and immunoblotting for Rac and Cdc42. Positive and negative controls (Cont) were prepared and run at the same time. (**C**) CSF-1-starved M–/–.WT and M–/–.Y721F cells were stimulated with 120 ng/ml CSF-1 for 0 or 30 seconds and lysates (Lys) subjected to GST–PAK–CRIB pull down for Rac-GTP and Cdc42-GTP followed by SDS-PAGE and immunoblotting for the indicated proteins. The arrow indicates the ~170 kDa phosphorylated protein, seen in M–/–.WT samples only.

Discussion

CSF-1 activation of the tyrosine kinase CSF-1R initiates a cascade of phosphorylation events to provoke a raft of cellular responses in macrophages, including gene transcription, protein translation and cytoskeletal remodeling (Pixley and Stanley, 2004). These induced responses transduce the pleiotropic effects of CSF-1 and require full expression of a wide range of signaling proteins, some of which are only expressed in mature macrophages grown in CSF-1 for up to a week (Martinez et al., 2006). Indeed, cytoskeletal and adhesion regulatory proteins are highly represented in the upregulated gene expression profile of CSF-1-induced BMM differentiation (Dinh et al., 2008). Thus, ectopic expression of the CSF-1R in non-macrophage cell lines cannot be used to examine normal macrophage signaling pathways, including those regulating motility. Moreover, model systems co-expressing mutant chimeric CSF-1Rs with WT receptors in macrophages do not permit examination of long-term (e.g. gene expression), as well as short-term, responses to signaling pathways activated by individual CSF-1R phosphorylated tyrosine motifs. Competitive interference by endogenous receptors can also occur with chimeric approaches. To address these issues, we have developed a novel system to express a single CSF-1R species in immortalized CSF-1R$^{-/-}$ BMMs (M–/– cells). M–/– macrophages expressing the WT receptor proliferate and differentiate normally in CSF-1, and morphologically resemble primary BMMs, whereas several cell lines expressing individual Y-to-F mutant receptors display obvious and distinct morphological abnormalities (e.g. M–/–.Y706F, M–/–.Y721F and M–/–.Y974F) (Yu et al., 2008). Although individual mutations of some of the remaining tyrosine residues might result in subtle morphological changes not evident by SEM (data not shown), here we have focused on characterization of the M–/–.Y721F cells.

Macrophages expressing the Y721F mutant CSF-1R look strikingly different to WT macrophages, with a loss of elongation and CSF-1-induced ruffling. Underlying this morphological change was a marked decrease in both the CSF-1-stimulated actin polymerization at 30 seconds and the formation of adhesions rich

in phosphorylated paxillin, which contributed to a substantial reduction in spreading and motility. Furthermore, this reduced motility in a two-dimensional in vitro environment is associated with a reduced infiltrative capacity in vivo and a reduced ability to promote carcinoma cell invasion. Thus, signaling pathways activated by phosphorylation of Y721 in the kinase insert of the CSF-1R regulate macrophage morphology and motility. In contrast to our findings, a recent study of osteoclasts and BMMs retrovirally transduced with erythropoietin (Epo)–CSF-1R chimeras reported that Y721 was dispensable for CSF-1 regulation of cytoskeletal remodeling and motility (Faccio et al., 2007); in their system the Y559-*P* motif was instead required for CSF-1-induced cytoskeletal remodeling and migration through recruitment of an SFK–Cbl–PI3K multimeric complex. An important difference between our system and that used by Faccio et al. is that we examined the effect of a single species of CSF-1R, either WT or mutant, in differentiated macrophages.

As Y721-*P*-initiated signaling regulates macrophage spreading and motility, immunoprecipitation analysis was performed to identify motility effectors associated with the Y721-*P* motif. Two known regulators of macrophage migration, PI3K and PLCγ2, have previously been shown to associate with the receptor, through Y721, in a phosphorylation-dependent manner (Reedijk et al., 1992; Faccio et al., 2007; Bourette et al., 1997). Here, we also show that Y721-*P* is required for direct association of p85 PI3K in our system. The association is rapid, prolonged and necessary for full activation of PI3K. In the absence of Y721, a late and weak association between PI3K and the receptor occurs, which could be mediated indirectly through either Y559-*P* and SFKs or Y974-*P* and Cbl (Faccio et al., 2007; Mancini et al., 2002). In contrast to PI3K, association of PLCγ2 with the CSF-1R was difficult to detect, had slower kinetics and was not dependent upon Y721. Similar results for PLCγ1 indicate that PLCγ-mediated macrophage motility signaling does not require Y721-*P*. Thus, although the association of other, as yet unidentified, motility effectors with the Y721-*P* motif cannot be ruled out, the striking loss of association of PI3K with the Y721F mutant CSF-1R strongly suggests that Y721-*P*-activated PI3K signaling regulates the early wave of actin polymerization and subsequent formation of adhesion structures to mediate CSF-1-induced spreading and motility in macrophages.

CSF-1 is one of many growth factors known to activate PI3K and stimulate a rapid rise in the levels of PtdIns(3,4,5)P_3 at the plasma membrane (Hawkins et al., 2006). Recent evidence suggests that PtdIns(3,4,5)P_3 regulates the rate, rather than the direction, of motility (Kolsch et al., 2008), which is consistent with our findings that chemokinesis and chemotaxis are similarly affected in M–/–.Y721F cells. PtdIns(3,4,5)P_3 signaling regulates motility and other cytoskeletal remodeling processes through recruitment and activation of PH-domain-containing proteins. Two PI3K pathways known to influence cell motility are PDK1-Akt signaling and Rac signaling. Mutation of Y721 slows the kinetics of Akt phosphorylation and activation, and reduces total activity, but there is still a robust Akt S473-*P* response and a substantial Akt T308-*P* response to CSF-1 stimulation. In M–/–.Y3AB cells, which lack signaling from all CSF-1R phosphorylated tyrosine residue motifs known to associate with signaling molecules except Y559, the Akt S473-*P* response is attenuated but substantially restored with add-back of Y721, whereas the Akt T308-*P* response is absent but only partially restored with Y721 add back. Taken together, these results indicate that the regulation of Akt signaling by CSF-1 is complex and that Akt is not activated solely through the direct association of PI3K with CSF-1R. Moreover, because mutation of Y721 severely affects CSF-1-induced motility, and restoration of Y721 on the Y3AB receptor returns chemotaxis to normal levels, pathways independent of Akt signaling appear to be mediating at least some of the Y721-*P*-stimulated motility. PDK1, the serine/threonine kinase responsible for activating Akt, activates a number of other AGC (protein kinase A, protein kinase G, protein kinase C family) kinases, such as isoforms of PKC, which might play a role in motility regulation (Pearce et al., 2010). However, as the ruffling response was almost completely abrogated in M–/–.Y721F cells, Rac was thought to be a more probable target for Y721-*P*-activated motility signaling. Using a GST–PAK–CRIB bead pull-down approach, we were surprised to find that not only could we not detect any differences between Rac activation levels in M–/–.WT and M–/–.Y721F cells, but that we could not demonstrate increased Rac or Cdc42 activation in response to CSF-1 stimulation at 30 seconds or at 3 minutes. Although a pull-down assay cannot detect localized Rac or Cdc42 activation, as is possible with a single cell assay such as fluorescence resonance energy transfer (FRET) (Gardiner et al., 2002), it is unlikely that we would be unable to detect a real increase in total cellular Rac-GTP or Cdc42-GTP at 30 seconds or 3 minutes in repeated replicate assays. Our data are consistent with previous reports that demonstrate Rac activation in macrophages occurs 5 minutes after stimulation and indicate that detectable activation occurs after the first wave of actin polymerization. Nevertheless, activated Rac or Cdc42 might still play a role in the early increase of actin polymerization through Y721-*P*-stimulated rapid and transient association of the ~170 kDa tyrosine-phosphorylated protein that we observed in the GTPase-GTP complex in M–/–.WT cells. In this circumstance, the GTPase could be acting as an adaptor protein. An extensive immunoblotting screen of ~170 kDa tyrosine-phosphorylated proteins, including PLCγ2 (Bunney et al., 2009) and Rac GEFs, such as Sos1, DOCK180, DOCK2, Arap3 and TIAM1, failed to identify the phosphorylated protein. Thus, signaling initiated by phosphorylation of CSF-1R Y721 triggers rapid PI3K association, phosphorylation and activation to stimulate an initial increase in actin polymerization at 30 seconds. This first wave of actin polymerization occurs at the same time as the ~170 kDa phosphorylated protein associates with either the Rac-GTP or Cdc42-GTP complex but in the absence of any detectable CSF-1-stimulated increase in Rac or Cdc42 activation, suggesting an alternative mechanism leads to the stimulation of actin polymerization in the early phase of the CSF-1 response.

These studies demonstrate that the CSF-1R Y721-*P* motif plays an important role in PI3K activation and PI3K and CSF-1R association upon CSF-1 stimulation. Signaling initiated by this motif stimulates adhesion and actin polymerization to regulate motility in macrophages, as well as their promotion of carcinoma cell invasion. Initial studies of the Y721-*P*-based motility pathways suggest they are partially independent of Akt activation and signal through regulation of interactions in Rac-GTP or Cdc42-GTP protein complexes. Further elucidation of these downstream pathways and identification of their crucial effectors could identify novel therapeutic targets to inhibit promotion of tumor progression and metastasis by tumor-associated macrophages.

Materials and Methods

Reagents

Antibodies used were monoclonal anti-phosphorylated-tyrosine (PY100), polyclonal anti-CSF-1R-Y721-*P* and anti-PLCγ1 antibodies and HRP-conjugated secondary antibodies (Cell Signaling), polyclonal anti-paxillin-Y118-*P* (Biosource, Invitrogen),

monoclonal anti-paxillin and anti-Pyk2 antibodies (BD Transduction Laboratories), polyclonal anti-p85-PI3K (06-497, Millipore), anti-PLCγ1 (Cell Signaling) and anti-PLCγ2 (Santa Cruz Biotechnology) antibodies and monoclonal anti-PtdIns(3,4,5)P_3 antibodies (Echelon Bioscience, Logan, UT). Alexa-Fluor-568-conjugated secondary antibody, Alexa-Fluor-568-conjugated phalloidin, Cell Tracker Red (CMTPX) cell labeling dye and Prolong Gold mounting solution were from Molecular Probes (Invitrogen).

Cell culture

M–/–.WT, M–/–.Y721F and other cell lines were cultured in supplemented alpha modified minimal essential medium (α+MEM) containing 10% newborn calf serum (NBCS; Invitrogen), as described previously. All lines were grown in 120 ng/ml human recombinant CSF-1 (a gift from Chiron Corporation, Emeryville, CA), for at least 1 week when thawed from GM-CSF-maintained stocks.

Microscopy

For immunofluorescent microscopy, macrophages were plated onto fibronectin-coated glass coverslips (BD Biosciences) and grown to 60–70% confluence in the presence of CSF-1. For CSF-1 stimulation experiments, cells were starved of CSF-1 for 7–16 hours before addition of CSF-1 (120 ng/ml) for indicated times. The cells were then rinsed with PBS and either sequentially fixed in 4% paraformaldehyde for 5–10 minutes and permeabilized with 0.25% Triton-X100 before staining for F-actin and paxillin Y118-*P* (1:100), as previously described (Pixley et al., 2005), or simultaneously fixed and permeabilized for 30 minutes in 3.7% paraformaldehyde, 0.1% glutaraldehyde and 0.15 mg/ml saponin before staining for F-actin and PtdIns(3,4,5)P_3 (1:250) as previously described (Yip et al., 2007). Epifluorescent samples were examined under an Olympus IX-81 inverted microscope with images recorded using a cooled FluoView II CCD digital monochrome camera. Quantification of cell polarization and cell footprint area were performed on either F-actin-stained or phase-contrast samples with polarization determined from the maximum length:maximum width ratio given by the 'best fit' ellipse for each cell, using ImageJ software. For this, and subsequent analyses, a two-sample *t*-test assuming unequal variance was used to determine statistical significance.

For TIRF microscopy, cells were treated as before and mounted in PBS then imaged with an inverted Nikon Ti E microscope and an 885 EMCCD camera using NIS elements software. For SEM, cells were fixed in 1% osmium tetroxide plus 0.1 M cacodylate for 5 seconds at 22°C followed by 2.5% glutaraldehyde plus 0.1 M cacodylate, as previously described (Pixley et al., 2001). Dehydrated cells were critical-point dried using liquid carbon dioxide in a Tousimis Samdri 790 critical point drier, sputter-coated with gold-palladium in a Denton Vacuum Desk-1 sputter coater, mounted and viewed in a JEOL JSM6400 scanning electron microscope using an accelerated voltage of 10 kV for SEM.

CSF-1 stimulation, immunoprecipitation and western blotting

Subconfluent (~70%) 100-mm dish cultures of cells were starved of CSF-1 for 16 hours to upregulate CSF-1R expression then incubated with 240 ng/ml CSF-1 at 37°C for the indicated times. Following incubation, cells were rinsed in ice-cold PBS, scraped into 200 μl of lysis buffer (1% NP-40, 10 mM Tris-HCl, 50 mM NaCl, 30 mM $Na_4P_2O_7$, 50 mM NaF, 500 μM Na_3VO_4, 5 μM $ZnCl_2$, 1 mM benzamidine, 10 μg/ml leupeptin and 10 μg/ml aprotinin, pH 7.2) at 4°C, vortexed and centrifuged at 13,000 ***g*** for 30 minutes. 500 μg of lysate was incubated with 2–5 μg of various antibodies and 40 μl of protein-G–Sepharose 4B beads (Zymed, San Francisco, CA) for at least 4 hours at 4°C, then centrifuged at 13,000 ***g*** for 30 seconds. After removal of the supernatant, beads were washed five times with wash buffer (lysis buffer with 0.5% NP-40 and no leupeptin or aprotinin) at 4°C and once in double-distilled water. Proteins were eluted in 3× XT sample buffer (10 μl) at 65°C for 15 minutes. SDS-PAGE and western blots were performed using the Criterion Bis-Tris XT gel electrophoresis system (Bio-Rad). Equal protein loading for lysates was confirmed by blotting with anti-GAPDH antibody (Abcam). Blotted membranes were incubated with HRP substrate (Millipore) and the chemiluminescent signal detected using Kodak Biomax film.

Quantitative RT-PCR

Total RNA was extracted from cells using the RNeasy protocol and reverse-transcribed using Omniscript reverse transcriptase according to the manufacturer's instructions (Qiagen). Mouse oligonucleotide primers were designed and synthesized (Sigma) for p85 PI3K (forward, 5′-AGCCGCCAGCTCTGATAATA-3′; reverse, 5′-TCTCCCCAGTACCATTCAGC-3′), PTPϕ (PTPRO) (forward, 5′- CTCCTGCA-ACACATTCGAGA-3′; reverse; 5′- AGGTATCATGTCCTCACCGC-3′), FAK (forward, 5′-ACATCTATCAGCCTGTGGGG-3′; reverse, 5′-GGCCAACTTC-CTTCACCATA-3′), Pyk2 (forward, 5′-TCCCCACACTAAACCTGGAG-3′; reverse, 5′-CACCGTACTGTGGACCTCCT-3′), PLCγ2 (forward, 5′-AACTGCG-GAGGCGGCAAGAA-3′; reverse, 5′-TCTCTCAGCCTCCGGTTGCACT-3′) and β-actin (forward, 5′-AGAGGGAAATCGTGCGTGAC-3′; reverse; 5′-CAATAGT-GATGACCTGGCCGT-3′). Real-time PCR was performed with SYBR Green Supermix (Bio-Rad) and amplification conditions as follows: initial step at 95°C for 3 minutes, followed by 40 cycles of 95°C for 10 seconds, 60°C for 60 seconds, and 72°C for 60 seconds. A melt temperature gradient curve was also constructed on samples by heating to 95°C for 60 seconds, 60°C for 60 seconds and then 81 cycles of increasing temperature in 0.5°C increments for 30 seconds each. Fluorescence was detected using an iQ5 Real Time PCR Detection System (Bio-Rad) and analyzed using the iQ5 Optical System Software (Bio-Rad). Samples were visualized with ethidium bromide on a 2% agarose gel to confirm a single amplicon of the correct size. Calculations of relative gene expression were performed with the $2^{-\Delta\Delta CT}$ method according to Pfaffl (Pfaffl, 2001), using β-actin as the control gene. Amplification efficiency was calculated using cDNA serial dilutions and negative controls were included for each gene of interest; at least three independent experiments were performed.

Motility assays

For time-lapse video microscopy, macrophages were plated on MatTek dishes (Ashland, MA) for at least 1 day before overnight removal of CSF-1. Cells were imaged by phase-contrast with a Nikon Diaphot inverted microscope with a heated chamber (Nikon) in Hepes-buffered medium with 10% NBCS for 5 minutes before CSF-1 was added to a final concentration of 120 ng/ml for a further 60 minutes. Images were taken every 15 seconds and cell movement was measured by centroid analysis of each cell in every tenth frame to determine total path length traveled per cell using ImageJ.

For Boyden Chamber motility assays, 2×10^5 cells were seeded into 8-mm pore size 24-well inserts (BD Biosciences) and the inserts placed in 120 ng/ml CSF-1 in normal medium in the lower wells. For chemokinesis assays cells were added in medium containing 120 ng/ml CSF-1, whereas cells were added in CSF-1-free medium for chemotaxis assays. Macrophages were allowed to migrate overnight before fixation in 4% paraformaldehyde and counting of cells on the underside of the insert membrane. The number of migrated cells was counted for ten fields per sample and normalized to the number of cells loaded. Assays were performed in triplicate in at least three independent experiments and results normalized to the control cells assayed for chemokinesis.

In vivo motility assays were performed in 5–6-week-old female BALB/c SCID mice inoculated 3–4 weeks previously with 1×10^6 GFP-expressing MTLn3 rat mammary carcinoma cells into the mammary fat pads (Kedrin et al., 2007). MTLn3 xenograft tumors (5–7 mm) were injected with 2×10^6 Cell Tracker Red (CPMTX)-labeled macrophages and the injection site marked. After 24 hours the animals were anaesthetized and the tumor exposed by dissection. The animals were placed on the pre-warmed (37°C) microscope stage, immobilized and imaged by multiphoton microscopy at the injection site for 1 hour using a Bio-Rad Radiance 2000 multiphoton microscope with an inverted Olympus IX-70 connected to a Spectra Physics Tsunami Ti:Sapphire laser. In vivo imaging experiments were performed according to the regulatory standards required by the animal welfare policy of the Institutional Animal Care and Use Committee of the Albert Einstein College of Medicine.

MTLn3 cell invasion assay

GFP-expressing MTLn3 carcinoma cells (8×10^4), in the presence or absence of macrophages (2×10^5), were cultured in a 35-mm MatTek dish in α-MEM with 10% FCS and 36 ng/ml CSF-1 for 16 hours (Goswami et al., 2005). The cultures were then overlaid with semi-soft collagen I (5–6 mg/ml) for 24 hours to allow cell invasion before fixation in 4% paraformaldehyde and imaging of optical *z*-sections using confocal microscopy, as described previously (Goswami et al., 2005). Quantification of MTLn3 cell invasion was calculated as the total GFP fluorescence measured >20 μm into the collagen layer divided by the sum of GFP fluorescence in all *z*-sections. Data were collected from triplicate samples with >200 cells per sample in three independent experiments.

F-actin polymerization assays

F-actin was quantified using an Alexa-Fluor-568–phalloidin-binding assay optimized for use in macrophages (Diakonova et al., 2002). Briefly, subconfluent cell cultures were starved of CSF-1 for 16 hours then re-stimulated with 240 ng/ml CSF-1 for the indicated times at 37°C. Following fixation in 3.7% formaldehyde and permeabilization in 0.2% Triton X-100, cells were stained for F-actin using saturating amounts of Alexa-Fluor-568–phalloidin (Invitrogen). Image acquisition was performed with IP Lab v3.51 (Scanalytics, Fairfax, VA) and analyses were performed with ImageJ. Mean fluorescence intensity of entire cells (50–100 cells per experiment) was measured at 20× and plotted against time after CSF-1 addition (Abou-Kheir et al., 2008).

Rac and Cdc42 activation assay

Activated Rac and Cdc42 assays were performed according to the manufacturer's instructions (Cytoskeleton, Denver, CO). Briefly, subconfluent cell cultures were starved of CSF-1 for 16 hours then re-stimulated with 240 ng/ml CSF-1 for either 0, 0.5 or 3 minutes before rinsing with ice-cold PBS and lysing in 200 μl of lysis buffer. Equal volumes of supernatants were incubated with GST–PAK–CRIB affinity beads for 1 hour at 4°C, followed by five washes in wash buffer. Bound proteins were eluted in 2× XT sample buffer and examined by SDS-PAGE in a 4–12% XT Bis-Tris gel and electrotransfer.

This work was supported by a National Health and Medical Research Grant 513817 (to F.J.P.), National Institutes of Health grants RO1 CA26504 (to E.R.S.), PO1 CA100324 (to D.C., J.C., E.R.S. and F.J.P.), R01 GM071828 (to D.C.), U54 CA126511 (to J.C.) and UO1 105490 (to J.W.). We thank Yee-Guide Yeung for his advice on biochemical procedures and Paul Rigby (Centre for Microscopy, Characterisation and Analysis, UWA) for his technical assistance with the microscopy protocols. Deposited in PMC for release after 12 months.

Supplementary material available online at
http://jcs.biologists.org/cgi/content/full/124/12/2021/DC1

References

Abou-Kheir, W., Isaac, B., Yamaguchi, H. and Cox, D. (2008). Membrane targeting of WAVE2 is not sufficient for WAVE2-dependent actin polymerization: a role for IRSp53 in mediating the interaction between Rac and WAVE2. *J. Cell Sci.* **121**, 379-390.

Allen, W. E., Jones, G. E., Pollard, J. W. and Ridley, A. J. (1997). Rho, Rac and Cdc42 regulate actin organization and cell adhesion in macrophages. *J. Cell Sci.* **110**, 707-720.

Boocock, C. A., Jones, G. E., Stanley, E. R. and Pollard, J. W. (1989). Colony-stimulating factor-1 induces rapid behavioural responses in the mouse macrophage cell line, BAC1.2F5. *J. Cell Sci.* **93**, 447-456.

Bourette, R. P., Myles, G. M., Choi, J.-L. and Rohrschneider, L. R. (1997). Sequential activation of phosphatidylinositol 3-kinase and phospholipase C-γ2 by the M-CSF receptor is necessary for differentiation signaling. *EMBO J.* **16**, 5880-5893.

Bunney, T. D., Opaleye, O., Roe, S. M., Vatter, P., Baxendale, R. W., Walliser, C., Everett, K. L., Josephs, M. B., Christow, C., Rodrigues-Lima, F. et al. (2009). Structural insights into formation of an active signaling complex between Rac and phospholipase C gamma 2. *Mol. Cell* **34**, 223-233.

Cheeseman, K. L., Ueyama, T., Michaud, T. M., Kashiwagi, K., Wang, D., Flax, L. A., Shirai, Y., Loegering, D. J., Saito, N. and Lennartz, M. R. (2006). Targeting of protein Kinase C-ε during Fcγ receptor-dependent phagocytosis requires the εC1B domain and phospholipase C-γ1. *Mol. Biol. Cell* **17**, 799-813.

Chitu, V. and Stanley, E. R. (2006). Colony-stimulating factor-1 in immunity and inflammation. *Curr. Opin. Immunol.* **18**, 39-48.

Condeelis, J. and Pollard, J. W. (2006). Macrophages: obligate partners for tumor cell migration, invasion and metastasis. *Cell* **124**, 263-266.

Diakonova, M., Bokoch, G. and Swanson, J. A. (2002). Dynamics of cytoskeletal proteins during Fcγ receptor-mediated phagocytosis in macrophages. *Mol. Biol. Cell* **13**, 402-411.

Dinh, H., Scholz, G. and Hamilton, J. A. (2008). Regulation of WAVE1 expression in macrophages at multiple levels. *J. Leukoc. Biol.* **84**, 1483-1491.

Epple, H., Cremasco, V., Zhang, K., Mao, D., Longmore, G. D. and Faccio, D. (2008). Phospholipase Cγ2 modulates integrin signaling in the osteoclast by affecting the localization and activation of src kinase. *Mol. Cell. Biol.* **28**, 3610-3622.

Faccio, R., Takeshita, S., Colaianni, G., Chappel, J., Zallone, A., Teitelbaum, S. L. and Ross, F. P. (2007). M-CSF regulates the cytoskeleton via recruitment of a multimeric signaling complex to c-fms Tyr-559/697/721. *J. Biol. Chem.* **282**, 18991-18999.

Fougerat, A., Gayral, S., Malet, N., Briand-Mesange, F., Breton-Douillon, M. and Laffargue, M. (2009). Phosphoinositide 3-kinases and their role in inflammation: potential clinical targets in atherosclerosis. *Clin. Sci.* **116**, 791-804.

Gardiner, E. M., Pestonjamasp, K. N., Bohl, B. P., Chamberlain, C., Hahn, K. M. and Bokoch, G. M. (2002). Spatial and temporal analysis of Rac activation during live neutrophil chemotaxis. *Curr. Biol.* **12**, 2029-2034.

Goswami, S., Sahai, E., Wyckoff, J., Cammer, M., Cox, D., Pixley, F., Stanley, E. R., Segall, J. and Condeelis, J. (2005). Macrophages promote the invasion of breast carcinoma cells via a CSF-1/EGF paracrine loop. *Cancer Res.* **65**, 5278-5283.

Gupton, S. L. and Waterman-Storer, C. M. (2006). Spatiotemporal feedback between actomyosin and focal-adhesion systems optimizes rapid cell migration. *Cell* **125**, 1361-1374.

Hawkins, P. T., Anderson, K. E., Davidson, K. and Stephens, L. R. (2006). Signaling through class I PI3Ks in mammalian cells. *Biochem. Soc. Trans.* **34**, 647-662.

Herrera-Velit, P. and Reiner, N. E. (1996). Bacterial lipopolysaccharide induces the association and coordinate activation of p53/56^{lyn} and phosphatidylinositol 3-kinase in human monocytes. *J. Immunol.* **156**, 1157-1165.

Jack, G. D., Zhang, L. and Friedman, A. D. (2009). M-CSF elevates c-Fos and phospho-C/EBPalpha(S21) via ERK whereas G-CSF stimulates SHP2 phosphorylation in marrow progenitors to contribute to myeloid lineage specification. *Blood* **114**, 2172-2180.

Kedrin, D., Wyckoff, J., Sahai, E., Condeelis, J. and Segall, J. E. (2007). Imaging tumor cell movement in vivo. *Curr. Protoc. Cell Biol.* **Chapter 19**, Unit 19.7.

Kheir, W. A., Gevrey, J. C., Yamaguchi, H., Isaac, B. and Cox, D. (2005). A WAVE2-Abi1 complex mediates CSF-1induced F-actin-rich membrane protrusions and migration in macrophages. *J. Cell Sci.* **118**, 5369-5379.

Kolsch, V., Charest, P. G. and Firtel, R. A. (2008). The regulation of cell motility and chemotaxis by phospholipid signaling. *J. Cell Sci.* **121**, 551-559.

Mancini, A., Koch, A., Wilms, R. and Tamura, T. (2002). c-Cbl associates directly with the C-terminal tail of the receptor for the macrophage colony-stimulating factor, c-Fms, and down-modulates this receptor but not the viral oncogene v-Fms. *J. Biol. Chem.* **277**, 14635-14640.

Martinez, F. O., Gordon, S., Locati, M. and Mantovani, A. (2006).Transcriptional profiling of the human monocyte-to-macrophage differentiation and polarization: new molecules and patterns of gene expression. *J. Immunol.* **177**, 7303-7311.

Owen, K. A., Pixley, F. J., Thomas, K. S., Vicente-Manzanares, M., Ray, B. J., Horwitz, A. F., Parsons, J. T., Beggs, H. E., Stanley, E. R. and Bouton, A. H. (2007). Regulation of lamellipodial persistence, adhesion turnover, and motility in macrophages by focal adhesion kinase. *J. Cell Biol.* **179**, 1275-1287.

Papakonstanti, E. A., Zwaenepoel, O., Bilancio, A., Burns, E., Nock, G. E., Houseman, B., Shokat, K., Ridley, A. J. and Vanhaesebroeck, B. (2008). Distinct roles of class IA PI3K isoforms in primary and immortalised macrophages. *J. Cell Sci.* **121**, 4124-4133.

Pearce, L. R., Komander, D. and Alessi, D. R. (2010). The nuts and bolts of AGC protein kinases. *Nat. Rev. Mol. Cell Biol.* **11**, 9-22.

Peifer, C. and Alessi, D. R. (2008). Small molecule inhibitors of PDK1. *Chem. Med. Chem.* **3**, 1810-1838.

Pfaffl, M. W. (2001). A new mathematical model for relative quantification in real-time RT-PCR. *Nucleic Acids Res.* **29**, 2002-2007.

Pixley, F. J. and Stanley, E. R. (2004). CSF-1 regulation of the wandering macrophage: complexity in action. *Trends Cell Biol.* **14**, 628-638.

Pixley, F. J., Lee, P. S. W., Dominguez, M. G., Einstein, D. B. and Stanley, E. R. (1995). A heteromorphic protein-tyrosine phosphatase, PTPϕ, is regulated by CSF-1 in macrophages. *J. Biol. Chem.* **270**, 27339-27347.

Pixley, F. J., Lee, P. S., Condeelis, J. S. and Stanley, E. R. (2001). Protein tyrosine phosphatase ϕ regulates paxillin tyrosine phosphorylation and mediates colony-stimulating factor 1-induced morphological changes in macrophages. *Mol. Cell. Biol.* **21**, 1795-1809.

Pixley, F. J., Xiong, Y., Yu, R. Y., Sahai, E. A., Stanley, E. R. and Ye, B. H. (2005). BCL-6 regulates RhoA activity to alter macrophage morphology and motility. *J. Cell Sci.* **118**, 1873-1883.

Reedjik, M., Liu, X., van der Geer, P., Letwin, K., Waterfield, M. D., Hunter, T. and Pawson, T. (1992). Tyr721 regulates specific binding of the CSF-1 receptor kinase insert to PI 3′-kinase SH2 domains: a model for SH2-mediated receptor-target interactions. *EMBO J.* **11**, 1365-1372.

Rohde, C. M., Schrum, J. and Lee, A. W. (2004). A juxtamembrane tyrosine in the colony stimulating factor-1 receptor regulates ligand-induced Src association, receptor kinase function, and downregulation. *J. Biol. Chem.* **279**, 43448-43461.

Songyang, Z., Shoelson, S. E., Chaudhuri, M., Gish, G., Pawson, T., Haser, W. G., King, F., Roberts, T., Ratnofsky, S., Lechleider, R. J. et al. (1993). SH2 domains recognize specific phosphopeptide sequences. *Cell* **72**, 767-778.

Takeshita, S., Faccio, R., Chappel, J., Zheng, L., Feng, X., Weber, J. D., Teitelbaum, S. L. and Ross, F. P. (2007). c-Fms tyrosine 559 is a major mediator of M-CSF-induced proliferation of primary macrophages. *J. Biol. Chem.* **282**, 18980-18990.

Van Rheenen, J., Song, X., van Roosmalen, W., Cammer, M., Chen, X., Desmarais, V., Yip, S. C., Backer, J. M., Eddy, R. J. and Condeelis, R. J. (2007). EGF-induced PIP2 hydrolysis releases and activates cofilin locally in carcinoma cells. *J. Cell Biol.* **179**, 1247-1259.

Weisberg, S. P., McCann, D., Desai, M., Rosenbaum, M., Leibel, R. L. and Ferrante, A. W., Jr (2003). Obesity is associated with macrophage accumulation in adipose tissue. *J. Clin. Invest.* **112**, 1796-1808.

Wilde, J. I. and Watson, S. P. (2001). Regulation of phospholipase C gamma isoforms in haematopoietic cells: why one and not the other? *Cell. Signal.* **13**, 691-701.

Wilhelmsen, K., Burkhalter, S. and van der Geer, P. (2002). c-Cbl binds the CSF-1 receptor at tyrosine 973, a novel phosphorylation site in the receptor's carboxy-terminus. *Oncogene* **21**, 1079-1089.

Wu, H., Yan,Y. and Backer, J. M. (2007). Regulation of class IA PI3Ks. *Biochem. Soc. Trans.* **35** (Pt 2) 242-244.

Wyckoff, J., Wang, W., Lin, E. Y., Wang, Y., Pixley, F., Stanley, E. R., Graf, T., Pollard, J. W., Segall, J. and Condeelis, J. (2004). A paracrine loop between tumor cells and macrophages is required for tumor cell migration in mammary tumours. *Cancer Res.* **64**, 7022-7029.

Yip, S. C., Eddy, R. J., Branch, A. M., Pang, H., Wu, H., Yan, Y., Dress, B. E., Neilsen, P. O., Condeelis, J. and Backer, J. M. (2008). Quantification of PtdIns(3,4,5)P_3 dynamics in EGF-stimulated carcinoma cells: a comparison of PH-domain-mediated methods with immunological methods. *Biochem. J.* **411**, 441-448.

Yu, W., Chen, J., Xiong, Y., Pixley, F. J., Dai, X. M., Yeung, Y. G. and Stanley, E. R. (2008). CSF-1 receptor structure/function in MacCsf1r–/– macrophages: regulation of proliferation, differentiation, and morphology. *J. Leukoc. Biol.* **84**, 852-863.